Progress In Electromagnetics Research Letters, Vol. 29, 75–86, 2012

COMPACT, PRINTED, STANDALONE PENTA-BAND ANTENNA FOR WWAN OPERATION

S.-W. Su* and Y.-W. Chang

Network Access Strategic Business Unit, Lite-On Technology Corporation, New Taipei 23585, Taiwan

Abstract—A standalone, printed monopole antenna with a two-branch shorting strip and a grounding wire to achieve a small size and yet multi-band operation for penta-band wireless wide area network (WWAN) operation (824–960/1710–2170 MHz) is presented. The antenna was formed on a low-cost, single-layered dielectric substrate with the dimensions 10 mm × 50 mm. By applying the proposed grounding wire and the dual-shorting strip, two resonant modes in close proximity in the antenna's lower band were obtained to cover the GSM850/900 operation. Further, the proposed shorting strip led to two additional, higher-order resonance excitation at about 1700 and 1800 MHz to assist in the formation of a wide upper band to cover the GSM1800/1900/UMTS operation. The proposed antenna also showed good radiation properties. Details of the design are described and discussed in the article.

1. INTRODUCTION

Compact and printed planar antennas capable of providing multi-band operation in the GSM850 (824–894 MHz), GSM900 (880–960), GSM1800 (1710–1880 MHz), GSM1900 (1850–1990 MHz), and UMTS (1920–2170 MHz) bands for wireless wide area network (WWAN) operation with the impedance-bandwidth requirement by a voltage standing wave ratio (VSWR) of 3 have recently been reported for wireless communications devices such as mobile phones [1–5] and laptops [6, 7] in the open literature. These printed antennas studied are all based on the antennas placed on or integrated with a large system/antenna ground plane to properly excite the antenna in the case of either the antenna as a matching element to couple to the

Received 27 November 2011, Accepted 27 December 2012, Scheduled 19 January 2012

* Corresponding author: Saou-Wen Su (susw@ms96.url.com.tw).

ground-plane resonance or the antenna to be the main radiator [8]. When the antenna ground plane is not allowed to be in contact with the system ground or liquid crystal display (LCD) ground in some industrial design (ID) situation, the standalone antenna solution is required accordingly. In this Letter, we propose a standalone, WWAN antenna design that shows a compact size of 10 mm × 50 mm, which was printed on a low-cost FR4 substrate, and was with a thin, flexible grounding wire of length 80 mm for practical applications. The design consists of a coupling monopole, a short-circuited monopole, a two-branch shorting strip, an L-shaped ground plane, and a thin grounding wire. The coupling monopole, the L-shaped ground, and the grounding wire mainly provide the fundamental and the higher-order resonance for GSM900 and UMTS operation. The shorted monopole is capacitively driven by the coupling monopole and has two resonant paths in the shorting strip. This element contributes to additional resonant modes in the GSM850 and GSM1800/1900 bands to combine with the aforementioned resonance, which makes it possible for two wide bandwidths achieved to cover the lower GMS850/900 MHz and the upper GSM1800/1900/UMTS bands. The proposed antenna was fed by mini-coaxial cable, which enables flexibility in the deployment inside a wireless device and avoidance of clashing with the predetermined mechanical configuration. The operating principle of the antenna will be described and discussed in detail. The experimental and simulation results are presented.

2. PROPOSED COMPACT PENTA-BAND ANTENNA

Figure 1(a) shows the proposed penta-band antenna formed on a single-layered FR4 substrate of thickness 1 mm and size 10 mm × 50 mm for WWAN operation. The design is mainly comprised of a coupling monopole, a short-circuited monopole, a two-branch shorting strip, an L-shaped ground plane, and a thin grounding wire. The grounding wire of length 80 mm is connected to the bottom left corner of the ground and used to obtain the resonance at about 940 MHz in the lower operating band. This conductive wire can be treated as part of the antenna ground for the main radiating element, too, and its length is about a quarter-wavelength at 940 MHz. The function of the coupling monopole, the L-shaped ground, and the grounding wire is similar to that of an unbalanced dipole with an offset signal feeding. These three elements also contribute to the higher-order resonant modes at about 2030 MHz in the upper band in addition to the fundamental mode at 940 MHz. Further, by incorporating a shorted monopole capacitively driven by the coupling monopole with a two-

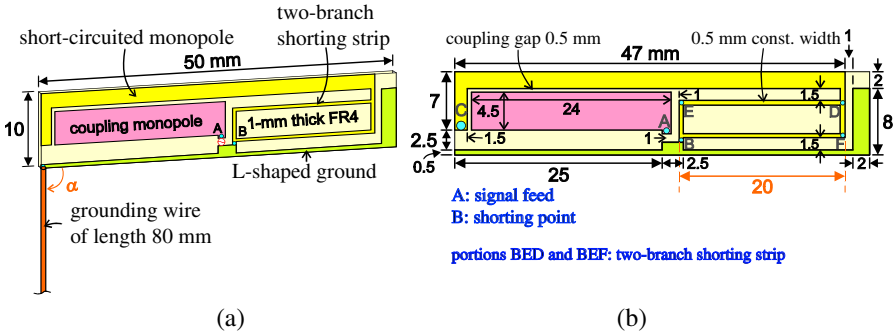

Figure 1. (a) Geometry of the compact, printed penta-band antenna for WWAN operation. (b) Detailed dimensions of the proposed antenna.

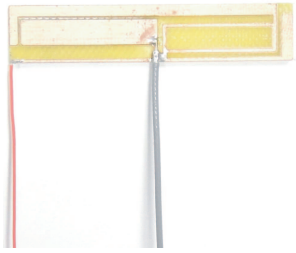

Figure 2. Photo of a design example fed by a 50-Ω mini-coaxial cable.

branch shorting strip, addition resonant modes can be obtained in the lower and the upper bands. This leads to two wide bandwidths covering the lower GMS850/900 MHz and the upper GSM1800/1900/UMTS bands. The length of the shorted monopole from points B to C corresponds to a quarter-wavelength at 800 MHz in general.

Figure 1(b) shows the detailed dimensions of the prototype. The antenna is of a long, narrow structure, which allows it to be placed in the space along the boundary with the grounding wire flexibly routed within a wireless device. The signal feeding for the coupling monopole is located at point A around the middle of the substrate, and the coupling monopole is encompassed by the shorted-monopole and the ground plane. The shorted-monopole is spaced 0.5 mm apart from the coupling monopole with its shorting point, point B, set close to the signal feeding. The feed gap between point A and the opposite antenna ground was fixed at 1 mm. The distance between the coupling monopole and the two-branch shorting strip was also tuned to be 1 mm. The resonant paths of the shorting strip can be separated into the routes $\overline{BED}$ and $\overline{BFD}$ respectively. Although the two routes are of the same length (of about 24 mm), they generate different resonance

at about 740 and 630 MHz in the lower operating band. The photo of a constructed prototype is demonstrated in Fig. 2, in which part of the grounding wire and the coaxial cable are cropped for better viewing. The wire utilized in this design is a common conductive wire that has an insulating sleeve outside. The coaxial cable is of the overall diameter (O.D.) 1.13-mm type with a miniature coaxial RF connector, commonly utilized to electrically couple the signals from the antenna to the WWAN module in practice. The preferred dimensions in this study were attained by the rigorous parametric studies with the aid of the electromagnetic-field simulation tool, Ansoft HFSS [9].

3. RESULTS AND DISCUSSION

Prototypes of the proposed antenna as shown in Fig. 2 were constructed and tested. Fig. 3 shows the measured and simulated return losses. On average, the measured data agree with the simulation results, which were based on the finite element method (FEM). Discrepancies were found due in part to printed-circuited-board manufacture tolerance and effects of coaxial cables in the experiments. Multiple resonant modes were excited with the impedance matching over the GSM850/900 and the GSM1800/1900/UMTS bands below a VSWR of 3. That's, the achievable antenna impedance bandwidth satisfies the practical specification for internal WWAN antenna designs.

The operating principle of the proposed antenna is discussed in Figs. 4 and 5. The return-loss characteristics of the three cases (reference antennas 1, 2, and 3) were analyzed; other dimensions remain the same as studied in Fig. 3. First, in the case of reference antenna 1, the antenna can generate the fundamental resonance at

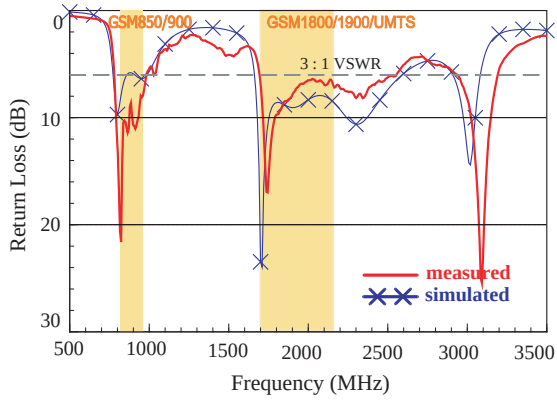

Figure 3. Measured and simulated return loss of the prototype; $\alpha = 90°$.

about 940 MHz and two higher-order resonant modes at about 2030 and 3050 MHz. The fundamental mode was considered being excited by an unbalanced dipole formed by the coupling monopole, the L-shaped ground, and the grounding wire with offset signal feeding. Second, by loading a shorted monopole capacitively driven by the coupling monopole with two different shorting-strip locations (see reference antennas 2 and 3), addition resonant modes can be obtained in the lower and the upper operating bands. The resonance at about 740 and 630 MHz by reference antennas 2 and 3 was seen shifted toward 800 MHz when the two shorting strips were consolidated, while the fundamental mode by reference antenna 1 was located at about the same frequency. This dual-resonance excitation in the lower band allows the antenna to cover the GMS850/900 MHz operation. Further, the higher-order modes at about 1820 and 1730 MHz by reference

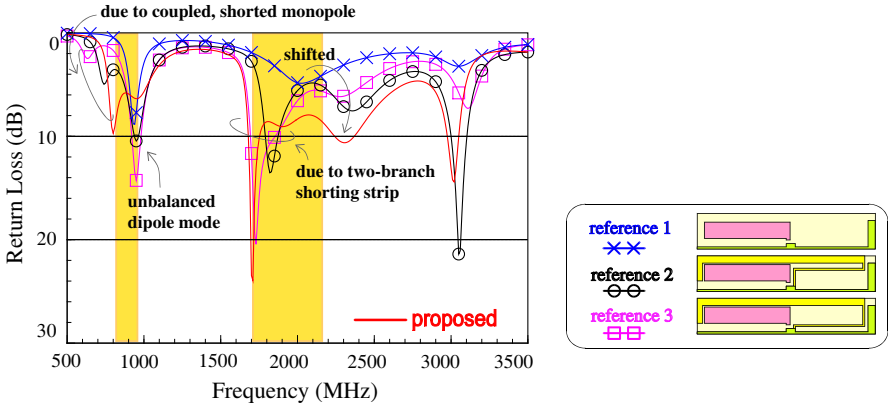

Figure 4. Comparison of the simulated return loss on the proposed design, the coupling monopole (reference antenna 1), the designs with a single shorting strip (reference antennas 2 and 3).

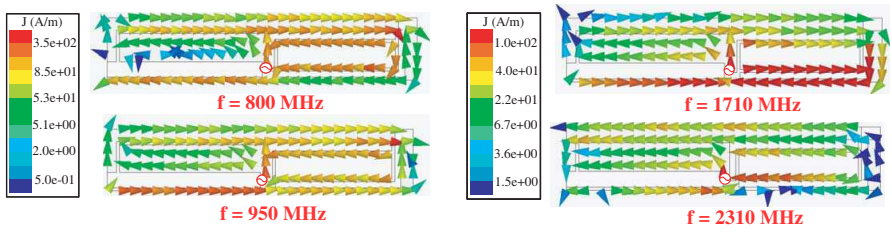

Figure 5. Simulated surface-current distributions at the four resonant modes at (a) 800 and 950 MHz and (b) 1710 and 2310 MHz for the antenna studied in Fig. 3.

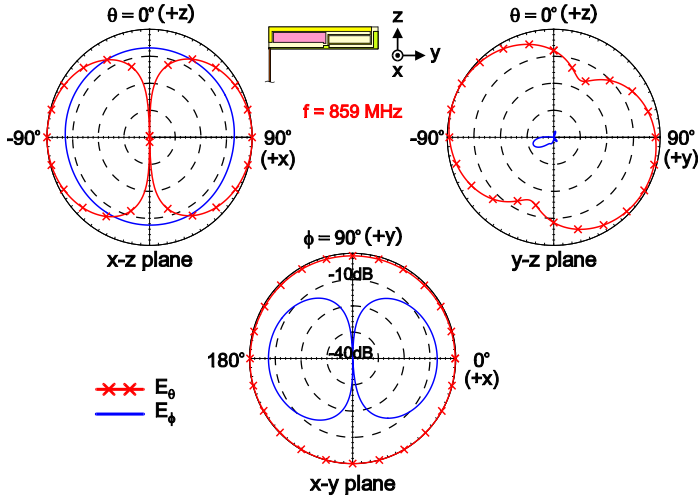

(a)

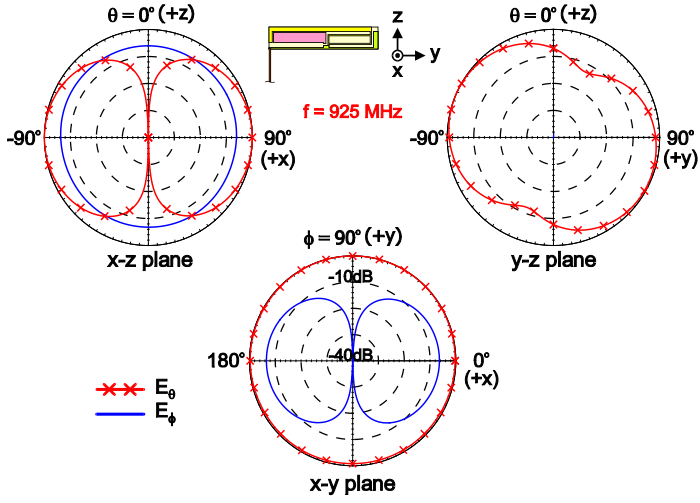

(b)

Figure 6. Simulated 2-D radiation patterns at (a) 859 and (b) 925 MHz.

antennas 2 and 3 were combined with the first higher-order mode by reference antenna 1. This leads to a wide bandwidth covering the upper GSM1800/1900/UMTS bands. Notice that the first higher-order mode by reference antenna 1 was moved toward 2310 MHz with better impedance matching.

The studies of the antenna surface-current distributions are presented in Fig. 5. Four resonant modes excited at 800, 950, 1710,

and 2310 MHz were chosen to also help illustrate the basic operating principle of the proposed design. The currents are plotted in the form of vectors (an arrow shape). For frequencies in the lower operating band shown in Fig. 5(a), larger current strength on the coupling monopole was seen at 950 MHz, corresponding to the fundamental mode of reference antenna 1 as discussed in Fig. 4. On the other hand, the currents at 800 MHz were greater on the shorted monopole, which is expected because this resonance was contributed to the coupled monopole with a two-branch shorting strip. For upper-band frequencies in Fig. 5(b), it can be seen that the current strength was larger on the shorting strip for the antenna excited at 1710 MHz. This phenomenon agrees with the return-loss properties of reference antenna 3 as described in Fig. 4. The current distributions for the other resonant mode at 1900 MHz were also confirmed to be produced by reference antenna 2; the results are not shown for brevity.

The over-the-air (OTA) performance of the prototype was studied. Figs. 6 and 7 shows the 2-D radiation patterns in E_θ and E_φ fields, and for brevity the patterns are only presented at the center frequencies of the five operating bands. Omnidirectional patterns were observed in the x-y plane. Dipole-like radiation patterns were found with tilted radiation null by about 26° and −30° with respect to the $+z$ axis as shown in the y-z plane (also see Figs. 8 and 11). The 3-D radiation patterns were measured in the ETS-Lindgren OTA test chamber using the great-circle method in a CTIA authorized test laboratory [10]; the results are given in Fig. 8. Other frequencies in the bands of interest were also measured, and good consistency in the patterns was observed. Fair agreement between the 3-D (measured) and the 2-D (simulated)

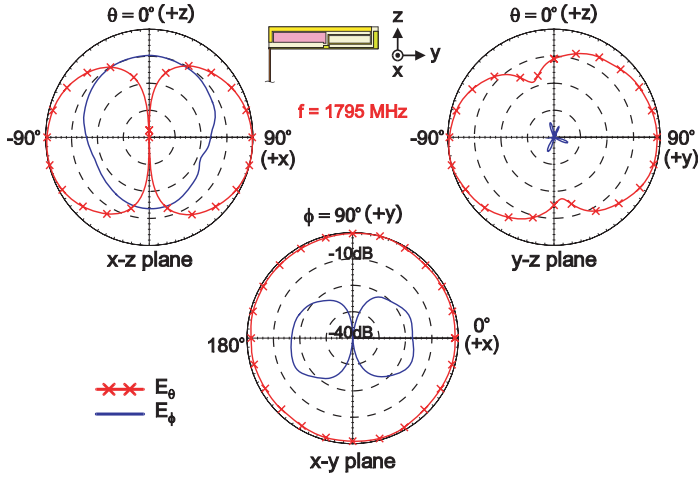

(a)

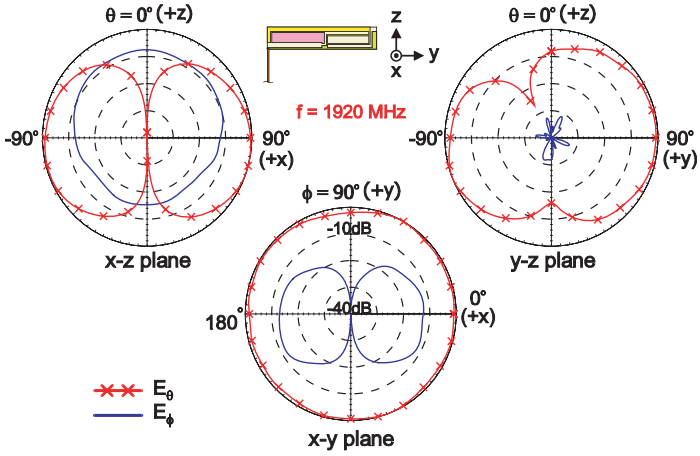

(b)

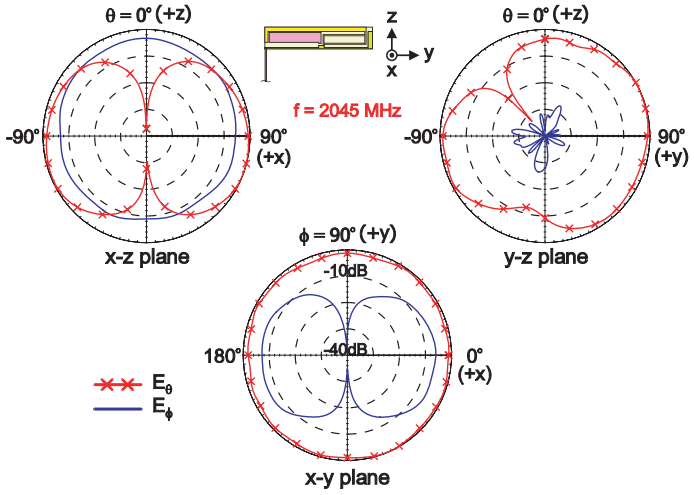

(c)

Figure 7. Simulated 2-D radiation patterns at (a) 1795, (b) 1920, and (c) 2045 MHz.

radiation patterns were also reached. Fig. 9 plots the measured, peak antenna gain and the radiation efficiency against frequency for the proposed antenna. The peak gain in the lower band varied from 0 to 2 dBi with the radiation efficiency of about 52%, which corresponds to the total radiated power (TRP) of −2.8 dBm when the given antenna input power is 0 dBm. For the upper band, the peak gain was in the range of 1.4 to 3.0 dBi with the radiation efficiency exceeding about 60%, corresponding to the TRP of −2.2 dBm. The peak-gain data

for each operating band are summarized in Table 1. The radiation efficiency was obtained by calculating the TRP of the antenna under test (AUT) over the 3-D spherical radiation first and then dividing that total amount by the input power of 0 dBm given to the AUT. Data points were taken every 15 degrees in the θ and ϕ axes, giving a total of 264 measurements for each polarization. The measurements at $\theta = 0$ and 180 degrees were not taken [11]. The gain measurement also took account of the mismatch of the antenna input impedance, and the "realized gain" [12] was measured.

Finally, Fig. 10 shows the simulated return loss for the antenna design with various angles of α. All resonant modes were spotted at similar frequencies as the angle varies. All the impedance bandwidth

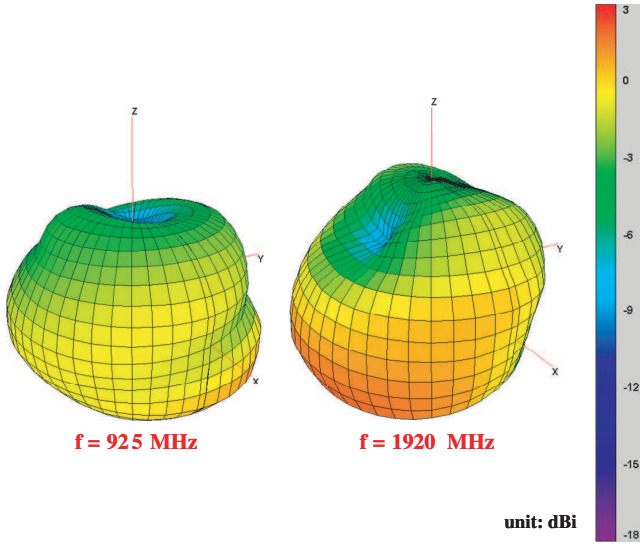

Figure 8. Measured 3-D radiation patterns for the prototype studied in Fig. 3 at 925 and 1920 MHz.

Table 1. Measured peak gain of the proposed antenna for each operating band.

WWAN Operation	Operating Band (MHz)	Peak Gain (dBi)
GSM850	824–894	0.7
GSM900	880–960	2.0
GSM1800	1710–1880	3.0
GSM1900	1850–1990	1.8
UMTS	1920–2170	2.6

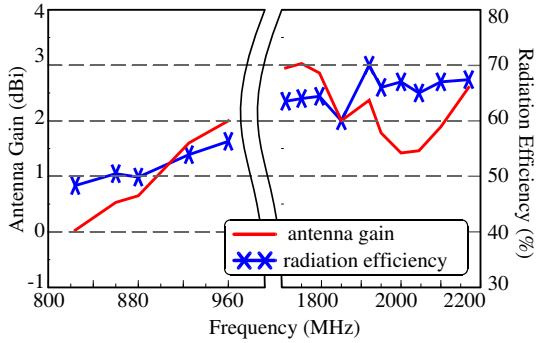

Figure 9. Measured antenna gain and radiation efficiency against frequency for the antenna studied in Figs. 8 and 9.

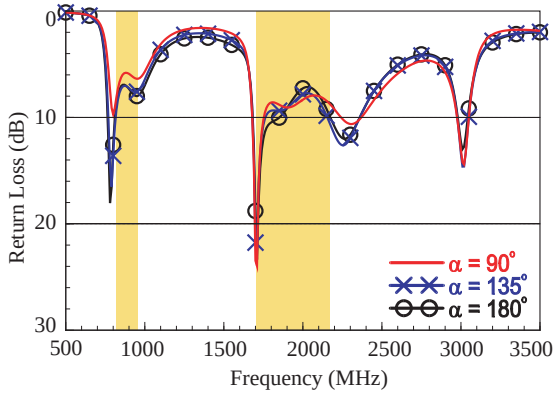

Figure 10. Simulated return loss for of the antenna as a function of the included angle α for the grounding wire. Other dimensions remain the same as studied in Fig. 3.

met the required specification. This suggests that the arrangement of the grounding wire can be very flexible with the penta-band operation still obtained. However, the grounding-wire routing can affect the radiation patterns and polarization thereof. For example, the simulated patterns at 925 and 1920 MHz with the angle α of 90° and 180° presented in Fig. 11 shows different radiation characteristics. Dipole-like patterns in the lower band were obtained for both cases in Fig. 11(a) with maximum field strength (omnidirectional plane) occurring in different cuts ($\theta = -67°$ and x-z plane for the case of $\alpha = 90°$ and 180° respectively). As for the cases in the upper band, the peak gain directions of the radiation were perpendicular to the grounding wire and different by about 90° between the two cases.

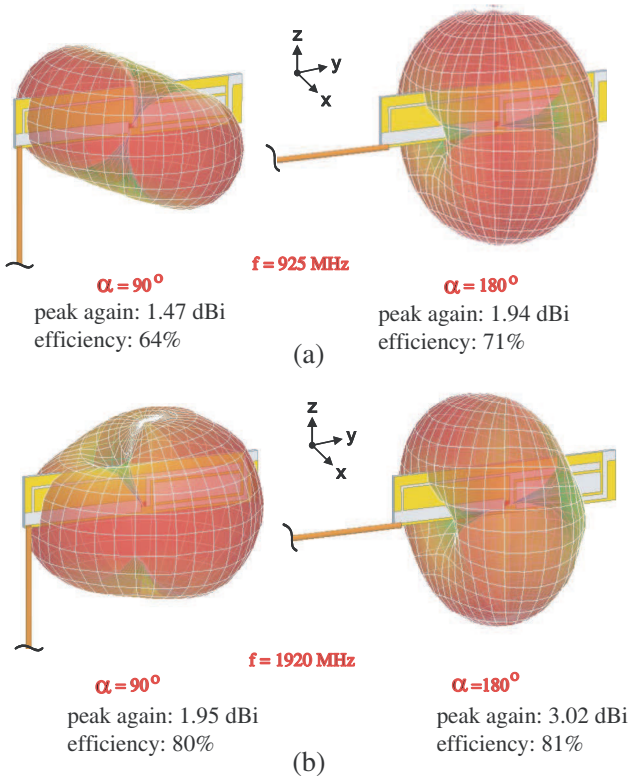

Figure 11. Simulated 3-D radiation patterns for the prototype studied in Fig. 3 with $\alpha = 0°$ and 90° at (a) 925 and (b) 1920 MHz.

4. CONCLUSION

A compact and printed monopole antenna formed on a small substrate of size 10 mm × 50 mm and capable of providing two wide operating bands for penta-band WWAN operation have been constructed, tested, and studied. The wide bandwidth was attained by the use of the grounding wire in combination with the two-branch shorting strip with no need of a large system/antenna ground plane. Good radiation characteristics with the radiation efficiency exceeding 50% and 60% over the lower and the upper operating bands were obtained. With the use of the coaxial-cable feeding, there exists much flexibility in the antenna placement within a limited space. The antenna can be mass-produced at low cost and is suitable for practical WWAN applications.

REFERENCES

1. Wong, K. L. and G. Y. Lee, "A low-profile planar monopole antenna for multiband operation of mobile handsets," *IEEE Trans. Antennas Propagat.*, Vol. 51, 121–125, 2003.
2. Lin, C. I. and K. L. Wong, "Printed monopole slot antenna for internal multiband mobile phone antenna," *IEEE Trans. Antennas Propagat.*, Vol. 55, 3690–3697, 2007.
3. Wong, K. L. and C. H. Huang, "Printed loop antenna with a perpendicular feed for penta-band mobile phone application," *IEEE Trans. Antennas Propagat.*, Vol. 56, 2138–2141, 2008.
4. Wong, K. L. and C. H. Huang, "Printed PIFA with a coplanar coupling feed for penta-band operation in the mobile phone," *Microwave Opt. Technol. Lett.*, Vol. 50, 3181–3186, 2008.
5. Chen, W. Y. and K. L. Wong, "Small-size coupled-fed shorted T-monopole for internal WWAN antenna in the thin-profile mobile phone," *Microwave Opt. Technol. Lett.*, Vol. 52, 257–262, 2010.
6. Wong, K. L. and L. C. Lee, "Multiband printed monopole slot antenna for WWAN operation in the laptop computer," *IEEE Trans. Antennas Propagat.*, Vol. 57, 324–330, 2009.
7. Wong, K. L. and S. J. Liao, "Uniplanar coupled-fed printed PIFA for WWAN operation in the laptop computer," *Microwave Opt. Technol. Lett.*, Vol. 51, 549–554, 2009.
8. Vainikainen, P., J. Ollikainen, O. Kivekas, and I. Kelander, "Resonator-based analysis of the combination of mobile handset antenna and chassis," *IEEE Trans. Antennas Propagat.*, Vol. 50, 1433–1444, 2002.
9. Ansoft Corporation HFSS, available at http://www.ansoft.com/products/hf/hfss.
10. CTIA Authorized Test Laboratory, CTIA, The Wireless Association, available at http://www.ctia.org/business_resources/certification/test_labs/.
11. Test Plan for Mobile Station over the Air Performance, Revision Number 2.22, 2008, available at http://files.ctia.org/pdf/CTIA_TestPlaforMobileStationOTAPerformanceRevision_2_2_2_Final_121808.pdf.
12. Volakis, J. L., *Antenna Engineering Handbook*, 4th Edition, Chap. 6, 16–19. McGraw-Hill, New York, 2007.